Evaluation of Slope Performance under Earthquake Loading Conditions

S. Rampello*, L. Callisto*, P. Fargnoli*

Summary

The response of slopes to earthquake loading may be studied via effective stress dynamic analyses, displacement-based sliding block analyses, or through force-based pseudo-static methods, the latter being the most widespread methods used in common practice. In the pseudo-static approach, an equivalent seismic coefficient k is used within a conventional limit equilibrium stability analysis. Since k designates the static force to be used in the calculations, its selection is crucial for stability assessment. In the paper, equivalent seismic coefficients are evaluated relating the ground motion amplitude to earthquake-induced slope displacements using a database of Italian strong-motion records. Influence of soil deformability, that results in spatial variation of the seismic motion within the slope, is also evaluated through two-dimensional seismic response analyses.

Keywords: Slope stability, Seismic performance, Earthquake, Seismic coefficient.

Introduction

An earthquake induces inertial forces that, combined with the pre-existing static forces, may reduce the stability of a slope. Because of the transient nature of earthquake loading, the main effects consist of permanent displacements induced either by a temporary mobilisation of the shear strength, or by irreversible strains activated by stress states distant from failure. Slope displacements may increase progressively during the earthquake, or be abruptly triggered during the ground motion. Moreover, these displacements can result either from strains diffused over the entire slope or from strain localisation within a limited failure zone.

Usually, significant slope displacements imply that the shear strength is mobilised in a significant portion of the slope. The available strength can also reduce during earthquake loading, due to pore water pressure increase or to degradation of shear strength parameters. Assuming undrained stress conditions during the seismic action, the shear strength can be expressed in the form:

$$\tau_f = c' + (\sigma'_n + \Delta\sigma_n - \Delta u) \cdot \tan\varphi' \qquad (1)$$

where σ'_n is the initial effective stress normal to the sliding surface, and $\Delta\sigma_n$ and Δu are the changes in total normal stress and in pore water pressure induced by earthquake loading. The effective cohesion, c', and the angle of shearing resistance, φ', may include eventual cyclic degradation. Significant reduction of shear strength may trigger slope failure with displacements developing after the end of the earthquake, under static conditions.

From the above discussion, it follows that slope instability is essentially driven by inertial effects and/or by a reduction in shear strength. Inertial forces are transient actions, that attain their maxima during strong motion. Conversely, shear strength reduction develops progressively, being mainly related to the development of excess pore water pressure and to cyclic degradation, and tends to be more important towards the end of the earthquake. Therefore, slope instability associated to inertial effects actually consists of displacements that cumulate during the earthquake, while instability induced by shear strength reduction may develop after the end of earthquake resulting in a static failure mechanisms.

Failure mechanisms caused by shear strength reduction may have different characteristics depending on soil behaviour, ductile or brittle, and soil type, coarse- or fine grained, as discussed by RAMPELLO and CALLISTO [2008]. These mechanisms can be analysed in the static condition following the seismic event, using conventional limit equilibrium methods, possibly accounting for the increase of pore water pressure and the degradation of strength parameters induced by earthquake loading.

On the contrary, when slope instability is induced by inertial forces, a progressive development of slope displacements occurs, that is limited to the duration of ground motion. Accordingly, the slope response to earthquake loading should be evaluated, in principle, using analysis procedures which ac-

* University of Rome La Sapienza – Department of Geotechnical and Structural Engineering

count for time-dependent seismic action and that allow an evaluation of displacements. If a pseudo-static approach is adopted to study this case, the seismic coefficient used in a limit equilibrium calculation must be calibrated against specified levels of slope performance, in turn defined by specified threshold values of earthquake-induced displacements. In the following, attention is focused on slope instability induced by inertial effects only, and on the appropriate choice of the seismic coefficient to use in the pseudo-static approach. A procedure is proposed in which the equivalent seismic coefficient is related to limiting slope displacements and to ground motion parameters.

Evaluation of equivalent seismic coefficients

The main difficulty in evaluating earthquake-induced slope displacements is the selection of acceleration time histories representative of site seismicity. In common practice, the seismic action is represented by a number of parameters that describe the main characteristics of ground motion (maximum horizontal acceleration, maximum velocity, Arias intensity etc.). Several parametric studies can be found in the literature in which permanent displacements computed using a given set of acceleration records are related to ground motion parameters and to the critical acceleration, that expresses the seismic vulnerability of the slope [FRANKLIN and CHANG, 1977; MAKDISI and SEED, 1978; AMBRASEYS and MENU, 1988]. By best-fitting the computed results, the proposed procedures provide conservative estimates of maximum expected displacements, for a given seismic input.

When using the pseudo-static approach, the seismic action is treated as an equivalent static force, which is proportional to the weight of the sliding soil through the seismic coefficient k. In the following, the seismic coefficient that in a pseudo-static analysis produces full strength mobilisation is termed the yield seismic coefficient k_y, while the peak value of the horizontal acceleration (normalized by g) spatially averaged within the slide mass is denoted by k_{max}.

The pseudo-static approach reduces the study of the seismic behaviour of a slope to the analysis of a static collapse mechanism. However, due to the transient and cyclic nature of seismic actions, the actual phenomenon is more similar to the progressive accumulation of displacements. Therefore, the seismic coefficient and the corresponding safety factor provided by the analysis have only a conventional meaning: their operational values should be determined through an equivalence with the actual seismic performance resulting from more adequate methods. This equivalence can be obtained using

relationships of the kind mentioned above between earthquake-induced displacements and given ground motion parameters.

Proposed simplified procedure

Simplified procedures have been proposed in the literature by SEED [1979] and HYNES-GRIFFIN and FRANKLIN [1984] for applications to earth dams, BRAY *et al.* [1998] for solid-waste landfills and STEWART *et al.* [2003] for hillside residential and commercial developments. All of them define an equivalent seismic coefficient k to calibrate the pseudo-static method to a particular level of slope performance, quantified by the earthquake-induced displacement.

In the following, a procedure is developed in which the horizontal seismic coefficient k and the corresponding safety factor F_S are evaluated using an equivalence with the results of a parametric application of the displacement method, as proposed originally by Newmark [1965]. In the procedure, the seismic coefficient is expressed as a function of the maximum acceleration of the sliding mass (k_{max}) and the limit displacement d_y accepted for the slope. The procedure is calibrated on earthquake magnitudes $M = 4 - 6.5$, typical of Italian seismic events.

The principle adopted to introduce a relationship between earthquake-induced displacements and corresponding seismic coefficients is schematically shown in Figure 1.

The permanent displacement d induced by an acceleration time history can be expressed as a decreasing function of the ratio k_y/k_{max}. For $k_y/k_{max} = 1$, the critical acceleration is never exceeded and, for a rigid-perfectly plastic soil, there are no permanent displacements. If the relationship between the
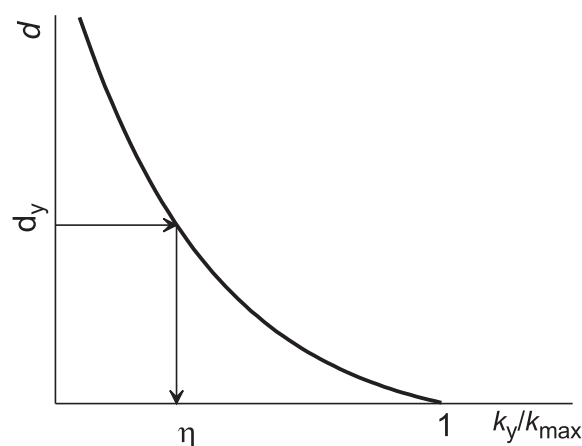

Fig. 1 – Equivalence between permanent displacement and seismic coefficient.
Fig. 1 – Equivalenza tra spostamenti indotti dal sisma e coefficiente sismico.

displacement d and the ratio k_y/k_{max} is known, for a given limit displacement d_y the corresponding value η of the ratio k_y/k_{max} can be obtained, as shown in Figure 1. If a pseudo-static analysis is carried out using $k = \eta \cdot k_{max}$ and the full mobilization of shear strength is obtained ($F_S = 1$), then it is $k = k_y$ and a permanent displacement equal to d_y can be anticipated for the slope. The equivalent seismic coefficient k is therefore the yield seismic coefficient that corresponds to the desired maximum displacement; it can be written as a fraction η of the maximum acceleration a_{max} for the sliding mass:

$$k = \eta \cdot k_{max} = \eta \cdot \frac{a_{max}}{g} \qquad (2)$$

where η decreases as the tolerable displacement increases.

In principle, the displacement method should employ an acceleration time history that in each time instant is equivalent to the distribution of inertial forces in the soil mass, and that therefore represents the overall dynamic response of the sliding mass. In the present approach, a rigid soil behaviour was assumed, which implies that, until full mobilisation of shear strength, the acceleration is uniform throughout the soil mass and can safely be taken equal to the acceleration at the ground surface. Site effects may be considered using the amplification factors for subsoil profile S_S and ground surface topography S_T specified by technical recommendations or building codes (e.g.: EN 1998-5, D.M. 14.01.2008); in Eq. (2) it is then $a_{max} = S_S \cdot S_T \cdot a_g$, where a_g is the peak acceleration at the rigid outcrop.

Permanent displacements were evaluated through a Newmark-type integration of a large set of acceleration time histories recorded during Italian earthquakes (database SISMA; SCASSERRA et al., 2008). A total of 214 time histories were used, recorded during 47 events by 58 stations. The acceleration time histories, all with a peak ground acceleration larger than 0.05 g, refer to earthquake magnitude $M = 4 - 6.5$, epicentral distance of 1 to 87 km, and focal depth in the range 2 – 24 km. They were coarsely divided into three groups, according to the subsoil classification provided by Eurocode 8 and by the Italian building code [EN 1998-5; D.M. 14.01.2008]: rock or rock-like subsoil, with shear wave velocity $V_S \geq 800$ m/s (A); dense granular and stiff cohesive subsoil, with $V_S = 360 - 800$ m/s (B); medium to loose granular and medium stiff to soft cohesive subsoil, with $V_S < 360$ m/s (C and D). Specifically, 74 records were attributed to subsoil class A, 98 to subsoil class B, and 42 to subsoil classes C and D.

For each group of accelerograms, peak accelerations were scaled to values of $a_{max} = 0.05$, 0.15, 0.25 and 0.35 g, excluding records that required scale factors outside the range 0.5 – 2. Displacements were computed integrating twice the equation of relative motion for translational sliding, using critical acceleration values from 10 to 80 % of the maximum acceleration ($k_y/k_{max} = 0.1 - 0.8$). Permanent displacements d computed for each subsoil class and for each level of acceleration are plotted in Figures 2, 3 and 4 as a function of the ratio k_y/k_{max} in a semi-logarithmic scale. Computed results were best-fitted using an exponential relationship:

$$d = B \cdot e^{A\frac{k_y}{k_{max}}} \qquad (3)$$

For each value of the ratio k_y/k_{max} it was assumed that the computed displacements are log-normally distributed.

In this hypothesis, the displacements corresponding to the 90th and the 94th upper-bound percentiles were obtained, and were interpolated again with equation (3), using the same parameter A of the average curves and values of $B_1 > B$ and $B_2 > B_1$. In the following, reference is made to the upper bound relationship corresponding to the 94th percentile.

For a given threshold displacement d_y, the corresponding values of η can then be obtained by inverting eq. (3) with $d = d_y$ and $B = B_2$:

$$\eta = \frac{k_y}{k_{max}} = \frac{\ln(d_y/B_2)}{A} \qquad (4)$$

Table 1 reports the values of η obtained for threshold displacements of 5, 15, 20 and 30 cm, corresponding to levels of damage from moderate to severe (Idriss, 1985).

Actually, the deformation pattern of a slope may differ from the simple sliding along a well defined surface, in that bulging or lateral spreading mechanisms may occur. Therefore, the threshold value of d_y should be considered just as a simple and approximated index of seismic performance of the slope.

Note that the present relationship between earthquake-induced displacements and seismic coefficients implies that a slope stability check, carried out with a limit equilibrium method and the proposed seismic coefficients, is satisfied even for $F_S = 1$. A value of F_S larger than one means that the slope has a critical acceleration larger than that corresponding to the limiting displacement d_y, and therefore it will undergo smaller seismic displacements.

Coefficients β_s reported by the Italian building code [D.M. 14.01.2008] for the pseudostatic analysis of slopes, reported in Table II, are based on the values of η listed in Table I. Although the code does note state the level of seismic performance associated to the use of β_s, a comparison between Tables I

subsoil class A

— median curve (*B*)
— 90th -percentile (*B₁*)
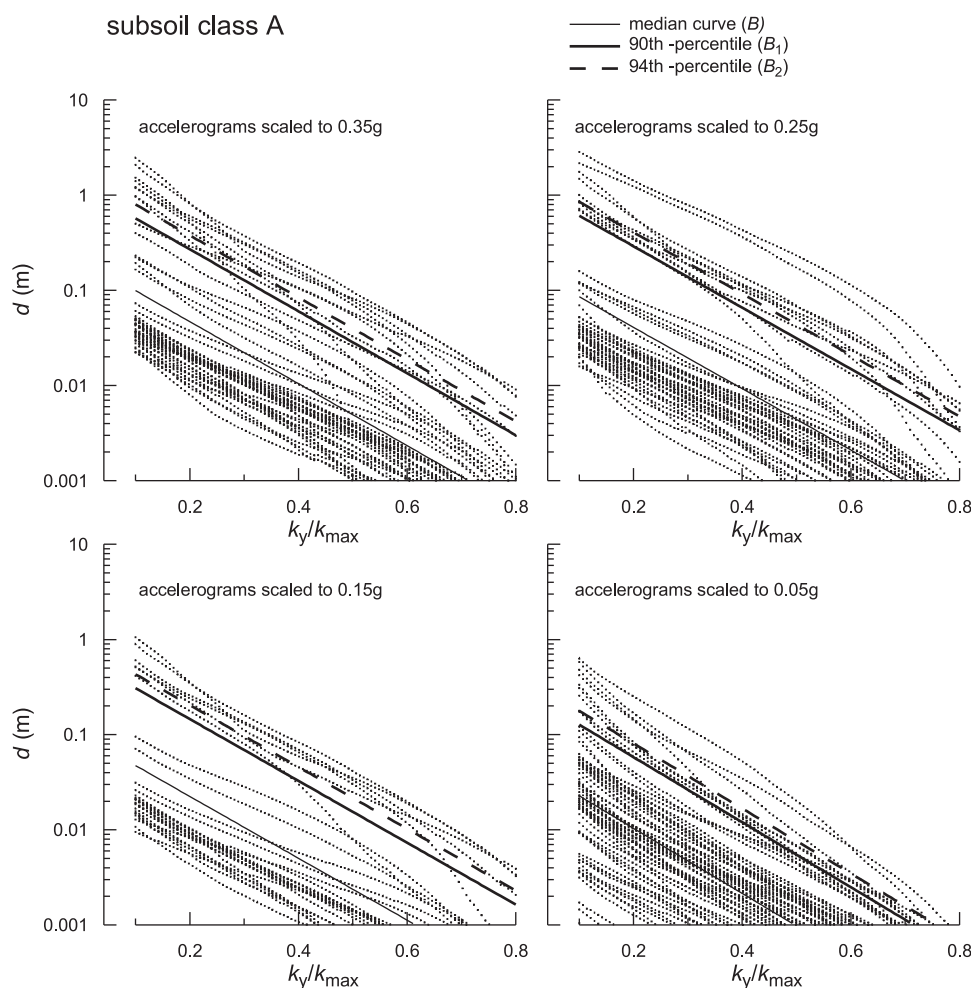— - 94th -percentile (*B₂*)

Fig. 2 – Permanent displacements computed using accelerograms recorded on subsoil class A
Fig. 2 – Spostamenti permanenti calcolati utilizzando accelerogrammi registrati su sottosuoli di categoria A.

Tab. II – Values of coefficient β_s versus acceleration level.
Tab. II - Valori del coefficiente β_s in funzione del livello di accelerazione (D. M. 14.01.2008).

	subsoil class	
	A	B, C, D, E
	β_s	β_s
$0.2 < a_g(g)$ 0.4	0.30	0.28
$0.1 < a_g(g)$ 0.2	0.27	0.24
$a_g(g)$ 0.1	0.20	0.20

and II reveals that the code provision corresponds to an expected seismic displacement (for $F_s = 1$) of ≈15–20 cm.

In general, displacements of 15 to 20 cm may be associated to low to moderate damage [IDRISS, 1985] and can be assumed as tolerable limit displacements for slopes. Moreover, it should be remembered that values of η were obtained from upper-bound best-fitting relationships.

Influence of sliding mass deformability

The procedure discussed above assumes an infinitely rigid sliding mass, associated to a uniform motion within the slope. More realistic descriptions of the seismic performance of slopes can be obtained taking into account the deformability of the sliding mass during ground motion, for instance using a de-coupled approach. In this approach, a seismic response analysis is first carried out to define an equivalent acceleration time history that accounts for soil deformability, and then this equivalent history is used to compute the displacements with a rigid-block sliding analysis [MAKDISI and SEED, 1978]. The seismic response analyses can be performed in one-dimensional (1D) or two-dimensional (2D) conditions, and the non-linear soil behaviour can be described through the equivalent linear approximation, that is known to yield a reasonable estimate of soil response at moderate levels of seismic intensity. In a seismic response analysis, spatial variation of the seismic forces within the slope is implicitly taken
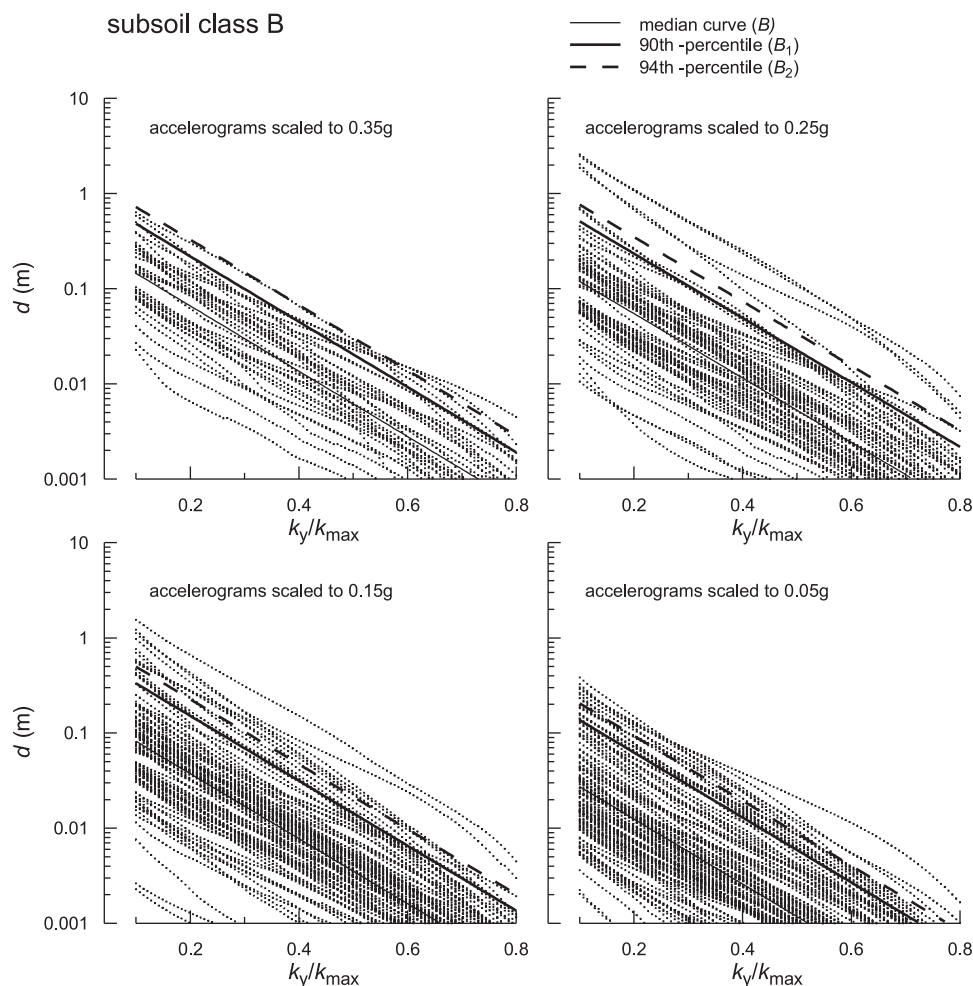
subsoil class B

Fig 3 – Spostamenti permanenti calcolati utilizzando accelerogrammi registrati su sottosuoli di categoria B.
Fig. 3 – Permanent displacements computed using accelerograms recorded on subsoil class B

into account, to a degree that depends on the accuracy of the 1D or 2D geometrical approximation of the slope.

In one-dimensional seismic response analyses, the sliding soil volume is regarded as a soil column with height H representing the depth of the sliding surface from the top of the slope. In this conditions, only vertical incoherence of seismic motion is accounted for, the inertial forces being assumed constant in the horizontal direction. Such an approximation is reasonable for steep slopes in which rotational sliding mechanisms characterised by low horizontal widths often occur (Fig. 5a).

More convincingly, two-dimensional seismic response analyses should be carried out to better represent slope geometry and to account for eventual focalisation of seismic waves near the crest of earth embankment or the top of slopes.

Two-dimensional seismic response analyses are also deemed necessary for shallow sliding mechanisms, characterised by low-curvature sliding surfaces, that often develop in gentle slopes. In these cases,

the horizontal width of the sliding soil volume is large and the change of the inertial forces along the horizontal direction cannot be neglected (Fig. 5 b).

In order to evaluate the influence of 2D seismic response on slope performance, the following section presents some results of a study in which the decoupled approach was applied to the evaluation of the seismic permanent displacements of idealised clayey slopes.

Problem geometry and soil properties

Translational sliding mechanisms were studied with reference to the simple scheme of an infinite slope with an inclination $\alpha = 20°$ and a water table at a depth $z_w = 5$ m from the ground surface. Three different depths D of the sliding surface were studied, equal to 5, 10, and 15 m. The length of the sliding soil volume, that is the distance between the alimentation and the accumulation zone, for which the approximation of the infinite slope is assumed, was $L = 5D$ and $10D$.
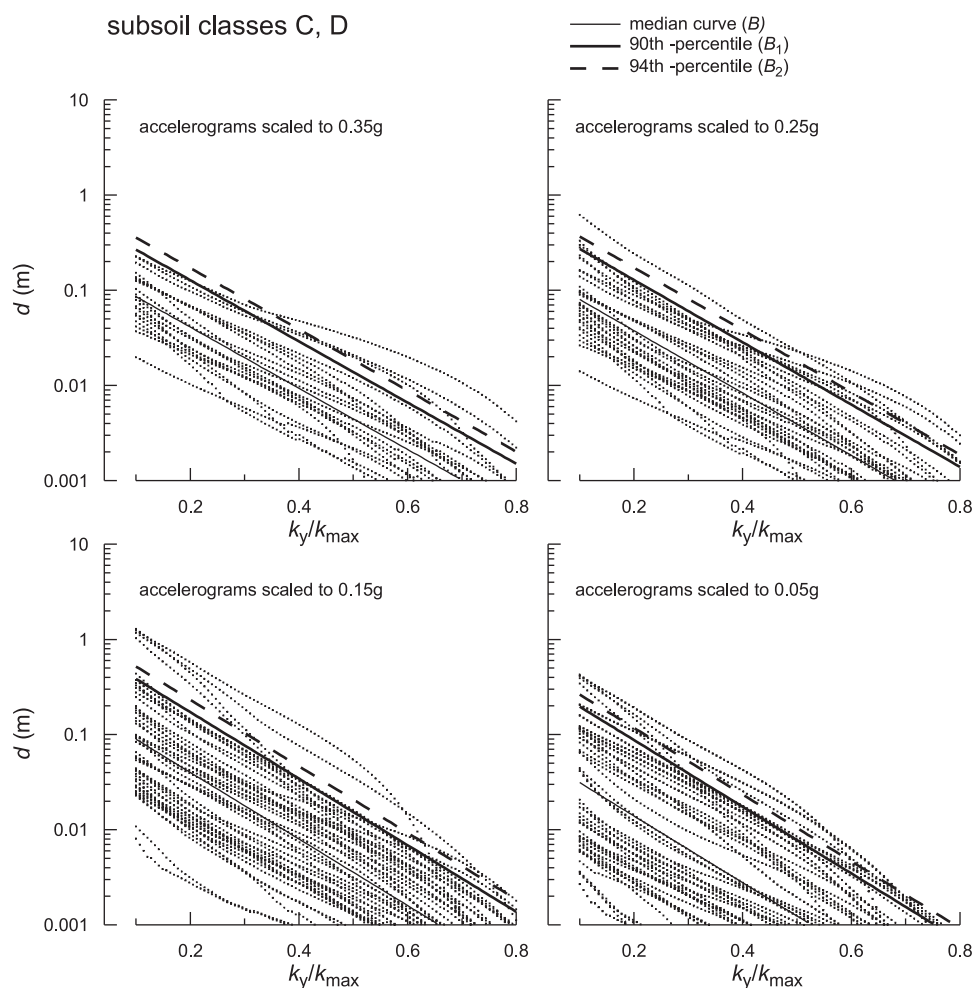
Fig. 4 – Spostamenti permanenti calcolati utilizzando accelerogrammi registrati su sottosuoli di categoria C, D.
Fig. 4 – Permanent displacements computed using accelerograms recorded on soil classes C, D.

Tab. I – Values of coefficient η versus threshold displacements.
Tab. I - Valori del coefficiente η in funzione degli spostamenti permanenti indotti dal sisma.

d_y (cm)	5	15	20	30	5	15	20	30	5	15	20	30
a_{max} (g)	η (subsoil class A)				η (subsoil class B)				η (subsoil class C, D)			
0.3 - 0.4	0.47	0.32	0.28	0.23	0.44	0.30	0.26	0.21	0.37	0.22	0.18	0.12
0.2 - 0.3	0.48	0.33	0.30	0.24	0.45	0.31	0.27	0.22	0.36	0.22	0.18	0.13
0.1 - 0.2	0.39	0.24	0.20	0.15	0.39	0.25	0.22	0.16	0.39	0.25	0.22	0.17
≤ 0.1	0.26	0.12	0.09	0.04	0.28	0.14	0.10	0.05	0.31	0.17	0.14	0.09

In these conditions, for angles of shearing resistance in the range $\varphi' = 21 - 28°$ and effective cohesions $c' = 0 - 0.05 \cdot \gamma D$, assuming a unit weight $\gamma = 19$ kN/m³, values of the critical seismic coefficient k_y are in the range 0.01 to 0.2.

Figure 6 (a) shows a scheme of the analysed domain. Starting from the toe of the slope, three groups of 6 sliding surfaces each were considered, located at increasing distance from the bedrock; such a distance, measured from the tip of the dee-

pest sliding surface, is $H = 15$, 66 and 118 m, respectively.

The seismic response analyses were carried out with the equivalent linear approach, in which the decay of the secant shear modulus and the increase of the damping ratio with the shear strain amplitude were taken from Vucetic and Dobry [1991] for a plasticity index $I_P = 25$ %. Both a medium-soft and a stiff clay deposit were considered, characteri-

Tab. III – Seismic parameters of input accelerogram.
Tab. III - Parametri sismici dell'accelerogramma di ingresso alle analisi.

event	record	M_w	H_{ipo} km	R_{epi} km	R_{jb} km	PGA g	T_m^{in} s	$D_{5\text{-}95}$ s	I_A m/s
Umbria Marche 12/10/97	NCB	5.2	6	11	6.2	0.186	0.128	4.13	0.158
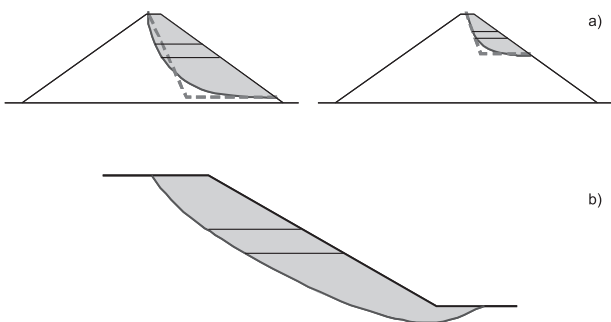
Fig. 5 – Slope schemes for seismic response analyses: (a) 1D analyses for steep and narrow mechanisms; (b) 2D analyses for shallow and wide sliding soil volumes.
Fig. 5 – Schemi di pendio per analisi di risposta sismica: (a) analisi 1D per pendii acclivi e superfici di scorrimento con angoli di immersione elevati; (b) analisi 2D in corrispondenza di creste e sommità e per cinematismi superficiali in pendii poco acclivi.

sed by a small-strain shear modulus G_0 depending on stress state and history [VIGGIANI, 1992]:

$$\frac{G_0}{p_r} = S \cdot \left(\frac{p'}{p_r}\right)^n R^m \qquad (5)$$

where p' is the mean effective stress; $p_r = 1$ kPa is a reference pressure; $R = p'_y/p'$ is the overconsolidation ratio, defined as the ratio of the mean effective yield stress p'_y to the current mean effective stress p'; S, n and m are non-dimensional stiffness

parameters. The stiffness exponents were evaluated as a function of the plasticity index using the empirical relationships proposed by RAMPELLO and VIGGIANI [2001]. Values of $n = 0.77$ and $m = 0.25$ were obtained for $I_P = 25$ % while $S_{nc} = 1200$, $R_{nc} = 1$ and $S_{oc} = 2500$, $R_{oc} = 10$ were adopted for the medium-soft and the stiff clay deposit, respectively. The corresponding profiles of the shear wave velocity V_S for the first 30 m below the ground surface are shown in Figure 6 (b).

Seismic input and analysis procedure

In the parametric study, earthquake loading was represented by 6 records of Italian seismic events selected from the database SISMA [SCASSERRA *et al.*, 2008] and recorded on very stiff outcrops in free field conditions. Specifically, the results described in this paper were obtained using the Borgo Cerreto Torre record (NCB 12/10/1997); Figure 7 shows the input acceleration time history and the corresponding Fourier amplitude spectrum. Table III summarises the main characteristics of the record; this is a near field, short signal, with high amplitude and high frequencies.

M_w = Magnitude; H_{ipo} = focal depth; R_{epi}: epicentral distance; R_{jb} Joyner and Boore distance; PGA = peak ground acceleration; T_m^{in} = mean qua-
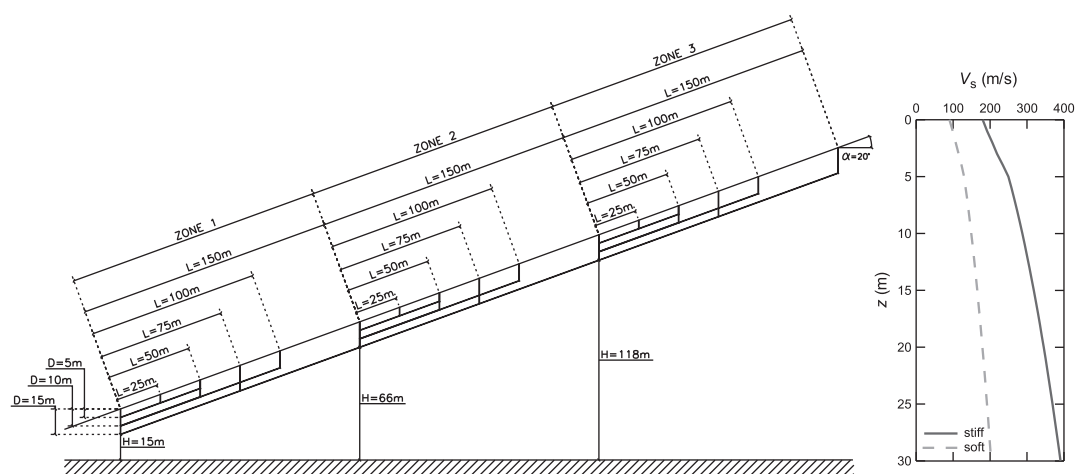

Fig. 6 – Scheme and position of the potentially sliding soil volumes (a) and assumed profiles of shear wave velocity (b).
Fig. 6 – Schema e posizione dei volumi di terreno potenzialmente instabili (a) e profili delle velocità di propagazione delle onde di taglio (b).
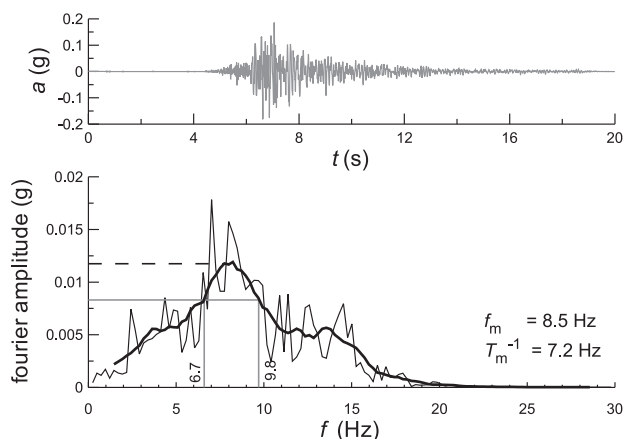
Fig. 7 – Input acceleration time history and Fourier spectrum.
Fig. 7 – Accelerogramma di ingresso alle analisi e spettro di Fourier in ampiezza.

dratic period; $D_{5\text{-}95}$ = significant duration; I_A = Arias intensity

Two-dimensional seismic response analyses were carried out with the finite element method using the code QUAKE. Due to the geometry of the analysed domain (see Fig. 6), to reduce the effects of waves reflected by the right vertical boundary, the FE mesh was extended to the right of the zone of interest for a length of 1200 m.

The boundaries of the FE mesh were fixed in the vertical direction; the time history of the horizontal acceleration was directly imposed to the lower boundary, thus simulating a perfectly reflecting bedrock. The input record was low-pass filtered to 15 Hz for compatibility with the mesh coarseness [LYSMER e KULHEMAYER, 1969].

For each soil volume, delimited by a potential sliding surface of length L, an equivalent horizontal accelerogram $a_{eq}(t)$ was computed starting from the instantaneous stress distribution along the sliding surface [CHOPRA, 1966]. Denoting with s (x, t) the stress vector acting on the sliding surface at time t and position x, and indicating with t_0 the initial instant, in which the stress state is lithostatic, the instantaneous horizontal inertial force (per unit length, in plane strain conditions) in the soil volume can be computed as:

$$\Delta f_x(t) = \int_S \left[s_x(x,t) - s_x(x,t_0) \right] dx \qquad (6)$$

where S is the sliding surface considered and s_x is the horizontal component of s. The equivalent acceleration was obtained by dividing this force by the mass m of the selected soil volume:

$$a_{eq}(t) = \frac{\Delta f_x(t)}{m} \qquad (7)$$

In computing the integral of equation (6) the contribution on the lateral sides of the soil volumes were neglected because of the high L/D ratio.

Seismic response of the idealized slopes

The histograms plotted in Figure 8 show the Arias intensity I_A, the maximum acceleration a_{max} and the average quadratic period T_m [RATHJE *et al.*, 1998] of the equivalent accelerograms computed for each sliding surface. Different shadings identify different groups of soil volumes, characterized by different bedrocks depths H. For each bedrock position H there are 3 depths D of the sliding surfaces and, for each depth D, there are 2 lengths L of the sliding surfaces. Increasing values of bedrock position (H), depth and length (D, L) of the sliding surfaces are encountered in the diagrams moving to the right.

The Arias intensity and the maximum acceleration of the equivalent accelerograms decrease with increasing size of the sliding soil volume, while the mean period increases with increasing values of L and D.

Compared with the input seismic parameters, smaller values of I_A and a_{max} are computed for the soft soil, while larger values are obtained in the stiff soil for shallow sliding mechanisms. In any case, a significant increase of the mean period T_m of the equivalent accelerograms is observed with respect to the corresponding values of the input seismic motion. The influence of the bedrock depth is less evident, although a slight increase of the above quantities is observed for the largest values of H, as a result of increasing amplification effects.

The results computed for a given input motion permit to relate the seismic performance of the slopes to the size of the potential sliding volume, to its position within the slope and to the stiffness of the soil deposit. All these quantities contribute in defining the ratio of the predominant wavelength of the seismic motion ($\lambda = V_s \cdot T_m^{in}$) to the size of the sliding soil volume (D, L). As this ratio becomes small, the instantaneous inertial forces in different zones of the selected soil volume have opposite signs and tend to cancel out, producing a decrease in the amplitude of the seismic motion. Basically, wavelength λ are smaller for input signals rich in large frequencies and by soil deposits with a low stiffness. Therefore, it can be anticipated that, for a given seismic input, earthquake effects will be larger for the stiff soil deposit and for the smallest size of the sliding volumes.

To substantiate these concepts, earthquake-induced displacements were computed for the different soil volumes using the equivalent accelerograms and a value of $K_y = 0.015$. The time-histories of these displacements are plotted in Figure 9. Thin lines refer to shallow sliding mechanisms ($D = 5$ m),
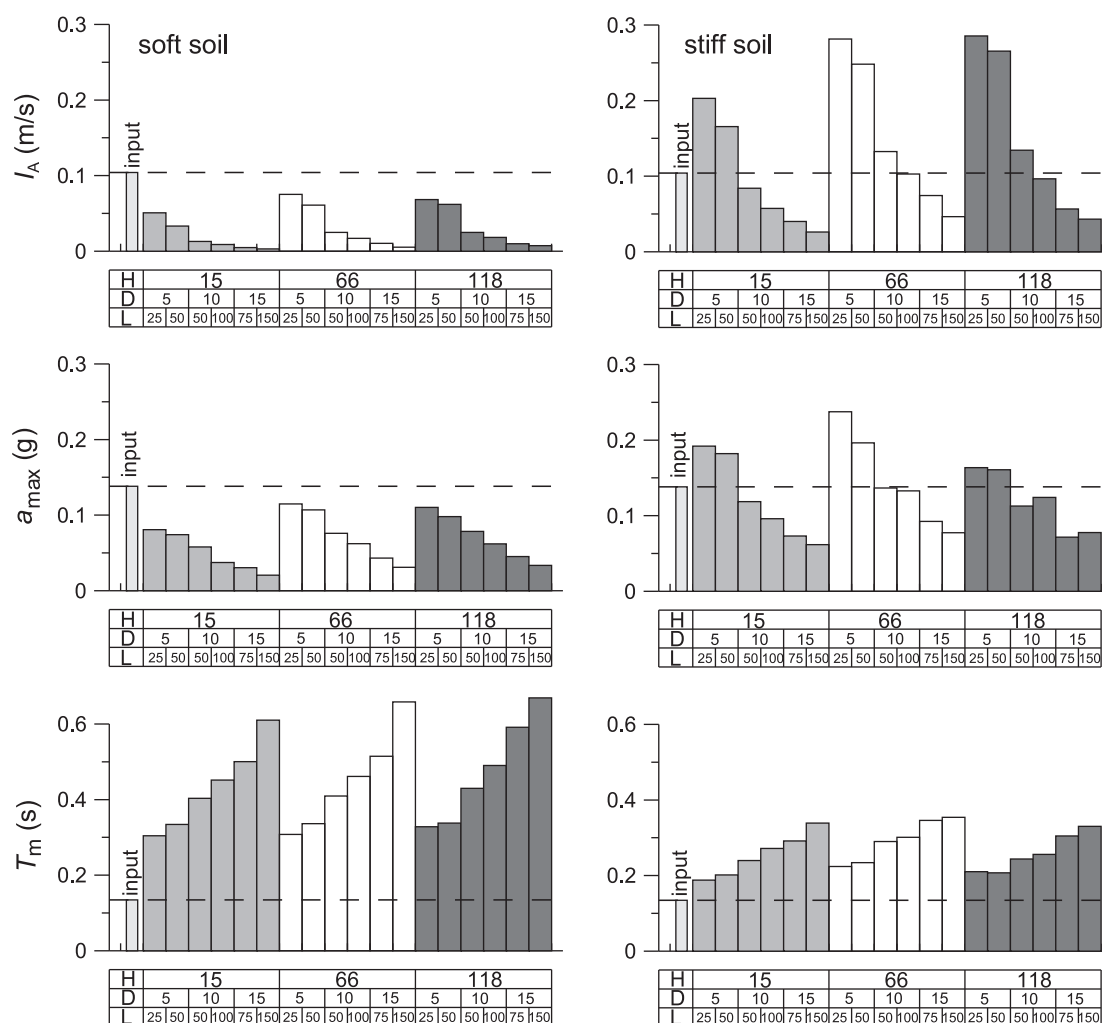
Fig. 8 – Properties of the equivalent accelerogram (I_A, a_{max} and T_m) for the different soil volumes considered in the analyses.
Fig. 8 – Proprietà degli accelerogrammi equivalenti (I_A, a_{max} e T_m) per i diversi volumi di terreno studiati.

thick grey lines to depths of sliding surfaces $D = 10$ m, while thick black lines are for deep mechanisms ($D = 15$ m). For each depth of the sliding surfaces, full lines are for short ($L = 25, 50, 75$ m) sliding mechanisms and the broken lines refer to long sliding surface ($L = 50, 100, 150$ m).

Diagrams to the left refer to the soft soil deposit, while those to the right are for the stiff soil deposit. The two plots on the top were obtained for a bedrock depth $H = 15$ m, the ones below are for $H = 118$ m.

It is seen that at the same values of D and L, displacements increase with increasing H and the increase is larger for the stiff soil. Also, for a given k_y, earthquake-induced displacements computed in the stiff soil are larger than the ones in the soft soil.

These observation could be attributed to amplification effects that become significant moving upwards in the slope and are more significant for a stiff soil.

On the contrary, computed displacements are seen to decrease with increasing size of the sliding volumes, and this can be related to asynchronous effects, that are more pronounced for the soft soil deposit. In this respect, the depth D of the sliding surface appear to have a stronger effect than the surface length L.

Alternatively, the displacements can be evaluated using the accelerogram computed, with the seismic response analysis, in a specific point that is assumed representative of the behaviour of the entire slope: for instance, at the centre of gravity of the potentially sliding mass. In this case, the subsequent displacement analysis assumes that the motion of the entire sliding mass is coincident with that computed at a single point.

Figure 10 shows a comparison between the earthquake-induced displacements evaluated using the accelerograms computed at the centre of gravity of the sliding masses, and those obtained using the equivalent accelerograms.
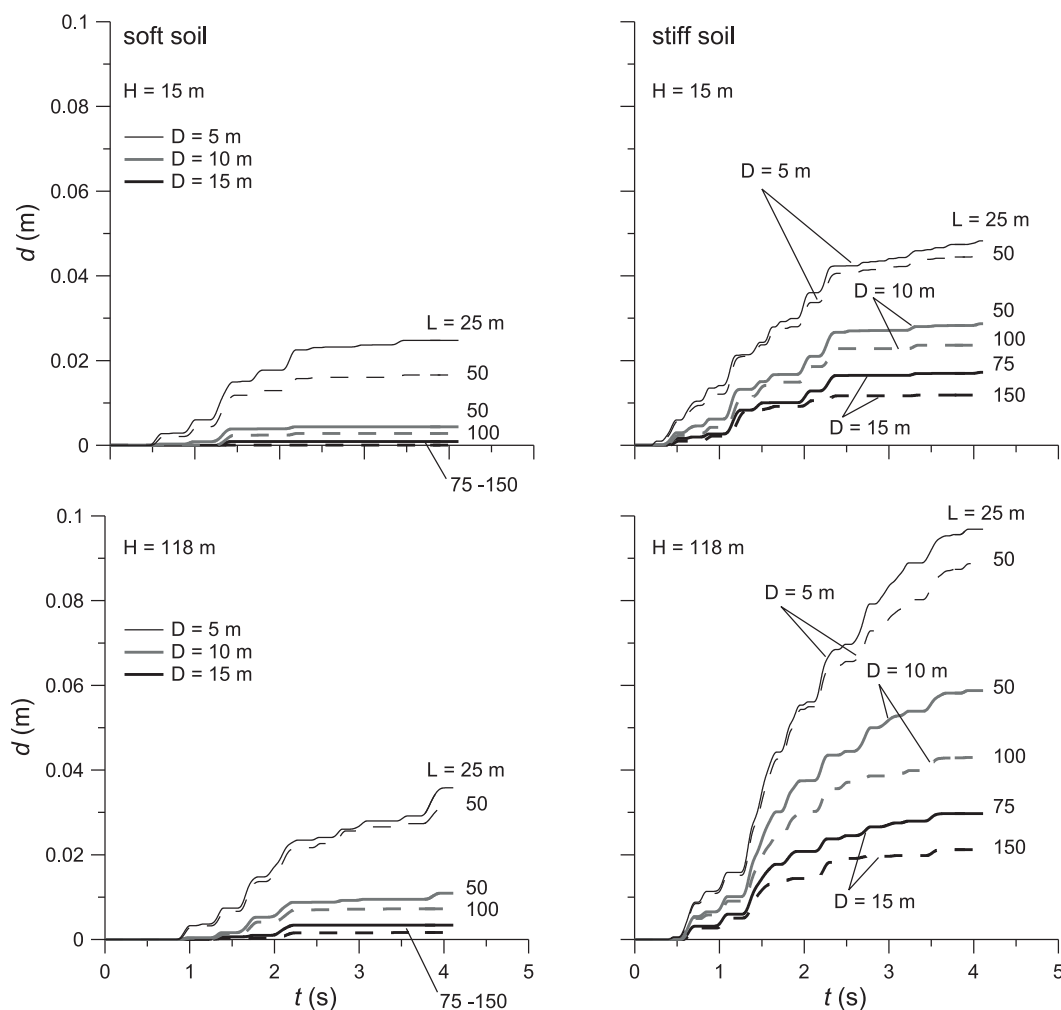
Fig. 9 – Time histories of permanent displacements computed integrating the equivalent accelerograms with $K_y = 0.015$.
Fig. 9 – Storie temporali degli spostamenti permanenti calcolati utilizzando gli accelerogrammi equivalenti per $k_y = 0.015$.

In this figure, displacement d are plotted as a function of the critical seismic coefficient k_y. Again, diagrams to the left are for the soft soil and those plotted to the right are for the stiff soil; upper diagrams show results obtained using the centre of gravity accelerograms, while the lower diagrams are obtained with the equivalent accelerograms. Open symbols refer to short sliding surfaces and full symbols are for long sliding surfaces; dotted lines indicate the obtained trend for shallow depths of the sliding surface, broken lines refer to values of $D = 10$ m and full lines to deep sliding surfaces.

It is seen that the use of the centre of gravity accelerogram for the evaluation of permanent displacements may be somewhat misleading. Neglecting the incoherence of the seismic motion, it is found that the longer sliding soil volumes undergo larger displacements than the shorter surfaces, because their centre of gravity is located uphill, where the effect of the focalisation of shear waves is more important. Conversely, accounting for the lack of synchro-

nicity in the seismic motion, i.e. using the equivalent accelerograms, it turns out that sliding volumes of increasing size undergo, as expected, smaller seismic displacements.

For the soft soil deposit, the equivalent accelerograms give displacements lower than the centre of gravity ones. For the stiff soil deposit, the centre of gravity time histories yield unrealistically large displacements, not related to the size of the sliding soil volume. On the contrary, when the equivalent accelerograms are used, displacements are smaller than the ones computed using centre of gravity accelerograms except for shallow and short sliding mechanisms, with a volume of the sliding mass smaller than the input predominant wavelength.

As a general result, the effects of an asynchronous soil motion become more important as the dimension of the sliding volume grows, causing larger gradients of the relationship between the computed displacements and the critical acceleration of the slope (Fig. 11).
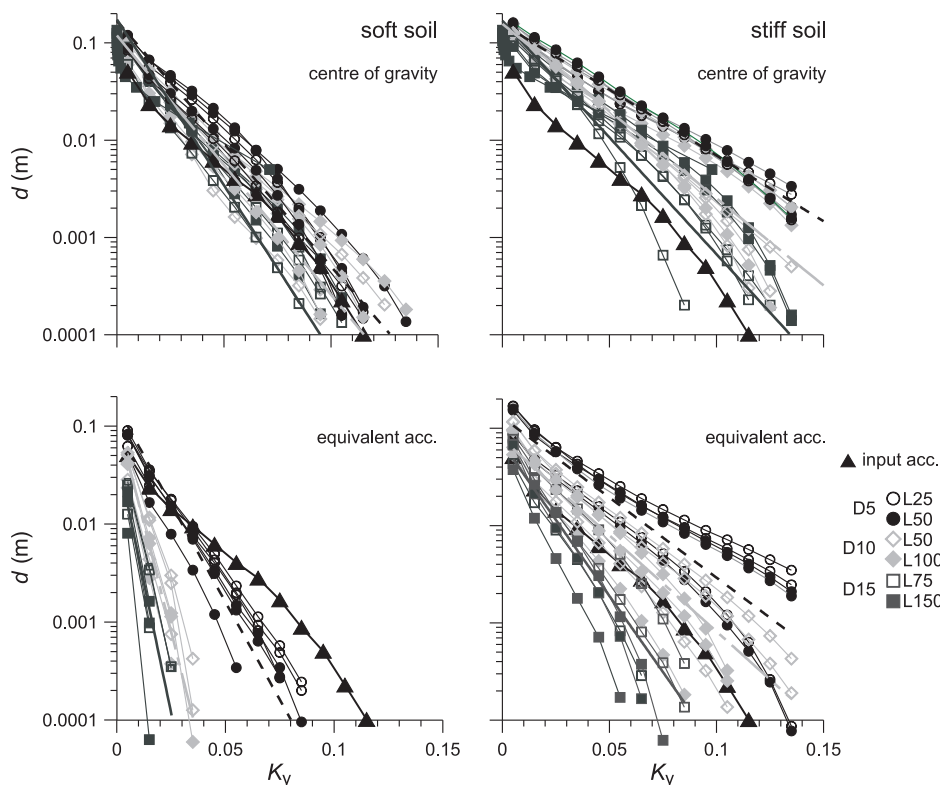
Fig. 10 – Permanent displacements computed integrating the equivalent accelerograms, plotted as a function of the critical seismic coefficient.
Fig. 10 – Spostamenti permanenti calcolati in funzione di k_y utilizzando gli accelerogrammi ottenuti nel baricentro dei volumi di terreno o gli accelerogrammi equivalenti.
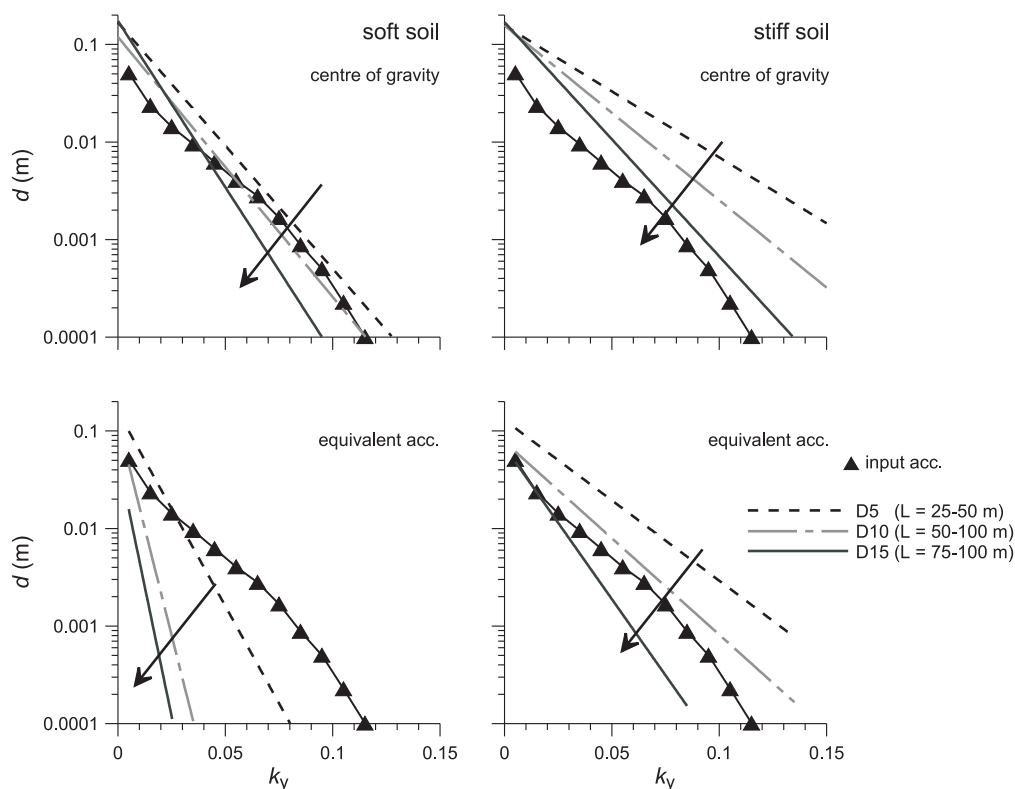

Fig. 11 – Influence of the size of the sliding soil volume on the earthquake-induced slope displacements.
Fig. 11 – Influenza della dimensione dei volumi di terreno potenzialmente instabili sugli spostamenti indotti dal sisma.

Conclusions

The seismic behaviour of a slope can be assessed using force-based or displacement-based procedures. In the force-based approaches, an equivalent seismic coefficient k is used in a conventional pseudo-static stability analysis to define the seismic demand E, which should not trespass the sliding strength resistance R (seismic capacity). If the seismic performance of a slope is expressed in terms of earthquake-induced displacements, the pseudo-static analysis may maintain its validity provided that the equivalent seismic coefficient k is evaluated with reference to a tolerable slope displacement.

In this work, a simple procedure was presented, in which the seismic coefficient k was expressed as a function of the maximum acceleration expected at the site, of the subsoil class, and of several given limiting slope displacements, related to the development of serviceability and ultimate limit states. The procedure was developed using acceleration time histories of Italian seismic events and assuming a rigid sliding mass. Values of k given in the Italian Building code [D.M. 14.01.2008] are similar to those obtained in this study for threshold displacements of 15-20 cm and should be used for the analyses of ultimate limit states. Serviceability limit states, associated to smaller acceleration levels, can tolerate smaller limit displacements. In this case, larger values of coefficient η should be used as the one associated to threshold displacement of 5 cm (Tab. I).

The influence of soil deformability was studied through two-dimensional seismic response analyses considering the simple case of translational sliding mechanisms characterised by sliding surfaces parallel to ground surface. Permanent slope displacements induced by an example earthquake loading were computed using a decoupled approach, evaluating equivalent accelerograms that represent the average seismic motion in the sliding soil volumes.

It was shown that, for a given yield acceleration, the slope displacements decrease as the sliding soil volume increases, and as the soil stiffness decreases, and this can be related to the development of an asynchronous motion within the soil mass. The quantities mentioned above contribute in defining the ratio of the predominant wavelength of the seismic event to the size of the sliding soil volume. As this ratio decreases, the instantaneous inertial forces tend to balance out, and the net inertial effect on the selected soil volume decreases, resulting in lower earthquake-induced displacements. Therefore, a realistic computation of the equivalent static forces in a deformable sliding masses should account for the frequency content of the earthquake and for the dynamic response of the soil.

References

AMBRASEYS N.N., MENU J.M. (1988) – *Earthquake-induced ground displacements*. Earthquake Engineering & Structural Dynamics, XVI, n.7, pp. 985 – 1006.
BRAY J.D., RATHJE E.M., AUGELLO A.J., MERRY S.M. (1998) – *Simplified seismic design procedure for geosynthetic-lined, solid-wasteland fills*. Geosynthetics International, 5, pp. 203–235.
CHOPRA A.K. (1966) – *Earthquake effects on dams*. Ph.D Thesis, University of California, Berkeley.
Decreto Ministeriale 14.1.2008 del Ministero delle Infrastrutture. *Nuove norme tecniche per le costruzioni*. S.O. n. 30 alla G.U. del 4.2.2008, n.29.
EN 1998-5. Eurocode 8: *Design of structures for earthquake resistance – Part 5: Foundations, retaining structures and geotechnical aspects*. CEN European Committee for Standardization, Bruxelles, Belgium.
FRANKLIN A.G, CHANG P.K. (1977) – *Earthquake resistance of earth and rockfill dams*. Report 5, Permanent displacement of earth embankments by Newmark sliding block analysis. MP S-71-17, Soils and Pavements Laboratory, US Army Waterways Experiment Station, Vicksburg, Miss.
HYNES-GRIFFIN M.E., FRANKLIN A.G. (1984) – *Rationalizing the Seismic Coefficient Method*. Miscellaneous Paper GL-84-13, Department of the Army, Waterways Experiment Station, Vicksburg, MS.
IDRISS I.M. (1985) – *Evaluating seismic risk in engineering practice*. Proc. 11th Int. Conf. on Soil Mechanics and Foundation Engineering, San Francisco, vol.I, pp. 255-320.
LYSMER J., KULHEMAYER R.L. (1969) – *Finite dynamic model for infinite media*. Journal of Engineering Mechanics, ASCE, vol. **95**, n. 4, pp. 859-877.
MAKDISI F.I., SEED H.B. (1978) – *Simplified procedure for estimating dam and embankment earthquake-induced deformations*. Journal of Geotechnical Engineering, ASCE, vol. CIV, pp. 849-867.
NEWMARK N.M. (1965) – *Effect of earthquakes on dam and embankment*. Géotchnique, vol. XV, n.2, pp. 139-160.
RAMPELLO S., CALLISTO L. (2008) – *Stabilità dei Pendii in condizioni sismiche*. In: Opere Geotecniche in condizioni sismiche. XII Ciclo di Conferenze di Meccanica e Ingegneria delle Rocce, pp. 241-271
RAMPELLO S., VIGGIANI G.M.B. (2001) – *Pre-failure deformation characteristics of geomaterials*. Discussion Leader Report on Session 1a: Laboratory tests.

Proc. 2nd Int. Symp. on "Pre-failure deformation characteristicsof geomaterials", Torino, Italy, Balkema, vol. II, pp. 1279-1289.

RATHJE E.M., ABRAHAMSON N.A., BRAY J.D. (1998) – *Simplified frequency content estimates of earthquake ground motions*. Journal of Geotechnical and Geoenvironmental Engineering, ASCE, vol.CXXIV, n. 2, pp.150-159.

SCASSERRA G., LANZO G., STEWART J.P., D'ELIA B. (2008) – *SISMA (Site Of Italian Strong-Motion Accelerograms): a web-database of ground motion recordings for engineering applications.* In: Seismic Engineering International Conference commemorating the 1908 Messina and Reggio Calabria Earthquake (MERCEA)*, Reggio Calabria, vol. II, pp.1649-1656.

SEED H.B. (1979) – *Considerations in the earthquake-resistant design of earth and rockfill dams. Géotechnique*, vol. XXIX, pp. 215–263.

STEWART J.P., BLAKE T.F., HOLLINGSWORTH R.A. (2003) – *A screen analysis procedure for seismic slope stability*. Earthquake Spectra, vol. XIX, n. 3, pp. 697-712.

VIGGIANI G.M.B. (1992) – *Small strain stiffness of fined grained soils*. PhD Thesis. City University, London, U.K.

VUCETIC M., DOBRY R. (1991) – *Effects of soil plasticity on cyclic response*. Journal of Geotechnical Engineering, ASCE, vol. CXVII**, n.1, pp. 89-107.

Valutazione della prestazione sismica dei pendii

Sommario

La valutazione del comportamento dei pendii in condizioni sismiche può essere eseguita mediante analisi dinamiche, nelle quali sia descritto realisticamente il comportamento meccanico dei terreni in condizioni cicliche; mediante i metodi degli spostamenti, portando in conto in maniera approssimata il carattere transitorio e ciclico dell'azione sismica; oppure, al livello più semplice e diffuso nelle applicazioni, mediante i metodi pseudostatici, in cui l'effetto dell'azione sismica è descritto da una forza statica equivalente di intensità proporzionale al peso del volume di terreno potenzialmente instabile, per il tramite del coefficiente sismico.

In molti casi il metodo degli spostamenti rappresenta un buon compromesso tra i metodi di analisi dinamica, che possono risultare eccessivamente onerosi, e i metodi pseudostatici, la cui attendibilità è fortemente dipendente dalla scelta del coefficiente simico.

Nell'ottica della progettazione prestazionale, l'analisi sismica di un pendio richiede una stima della sua prestazione, quasi sempre definita in termini di spostamenti permanenti indotti dal terremoto. Anche l'impiego dei metodi pseudostatici deve condurre ad una stima, ancorché indiretta, della prestazione sismica del pendio. A questo fine, i valori del coefficiente sismico da utilizzare in un'analisi pseudostatica devono essere correlati a fissati valori di spostamento.

In questo lavoro si propone una procedura semplificata per l'analisi sismica dei pendii basata sul metodo pseudostatico, nella quale il coefficiente sismico è valutato sulla base di un'equivalenza con i risultati ottenuti da un'applicazione parametrica del metodo degli spostamenti. In particolare, il coefficiente sismico è definito in funzione della massima accelerazione agente sul corpo di frana, del rapporto tra l'accelerazione critica e l'accelerazione massima (k_y/k_{max}) e dell'entità degli spostamenti ritenuti tollerabili per il pendio. La corrispondente verifica pseudostatica è soddisfatta per valori del coefficiente di sicurezza maggiori o uguali all'unità. La procedura proposta è riferita a valori della magnitudo M = 4 – 6.5, tipici di eventi sismici italiani, ed è stata calibrata su un insieme di 214 registrazioni accelerometriche (nelle 3 componenti) suddivise in tre gruppi, in funzione dei valori della velocità di propagazione delle onde di taglio nel sottosuolo dei siti di registrazione: sottosuoli di categoria A, di categoria B e di categoria C e D [D. M. 14.01.2008].

Si mostra che il valori del rapporto fra il coefficiente sismico e l'accelerazione massima forniti dalle Norme Tecniche per le costruzioni [D.M. 14.01.2008] sono attribuibili a intervalli di spostamenti permanenti indotti dal sisma di 15 – 20 cm; essi devono quindi essere utilizzati per le verifiche nei confronti degli stati limite ultimi. Le verifiche per gli stati limite di esercizio, associati a minori livelli di accelerazione, prevedono invece soglie limite di spostamenti più basse (es. 5 cm) e conseguentemente, valori maggiori del suddetto rapporto (Tab. I).

Per valutare l'effetto della deformabilità del corpo di frana sulla prestazione sismica dei pendii, si sono infine eseguite delle analisi di risposta sismica, svolte in condizioni di deformazione piana, per lo studio del comportamento sismico di volumi di terreno caratterizzati da diversi rapporti tra lunghezza e profondità della superficie di scorrimento e da cinematismi paralleli al piano campagna, riconducibili al semplice schema di pendio indefinito. Gli spostamenti indotti dal sisma sui volumi di terreno analizzati sono stati valutati mediante l'approccio disaccoppiato, utilizzando gli accelerogrammi equivalenti che rappresentano il comportamento d'insieme del volume potenzialmente instabile in condizioni sismiche.

Per una fissata soglia di accelerazione critica, gli spostamenti calcolati decrescono al crescere delle dimensioni del corpo di frana e al decrescere della rigidezza dei terreni che costituiscono il pendio, per il progressivo sviluppo di effetti di moto asincrono, ovvero dell'incoerenza spaziale del moto sismico all'interno del corpo di frana. Il comportamento atteso può essere correlato al rapporto tra le lunghezze d'onda predominanti dell'evento sismico di ingresso ($\lambda = V_s \cdot T_m^{in}$) e le dimensioni del volume di terreno potenzialmente instabile. Al decrescere di tale rapporto, le forze di inerzia istantanee tendono ad annullarsi e l'azione inerziale netta agente nel corpo di frana si riduce, con una conseguente riduzione degli spostamenti indotti dal sisma. Ne consegue che una valutazione più realistica, anche se concettualmente meno cautelativa, delle forze statiche equivalenti al sisma dovrebbe portare in conto il contenuto in frequenza dell'evento sismico e la risposta sismica dei terreni costituenti il pendio.